

SIMULATION OF SURFACE MUON BEAM LINE, ULTRASLOW MUON PRODUCTION AND EXTRACTION FOR THE J-PARC G-2/EDM EXPERIMENT

M. Otani*, N. Kawamura, T. Mibe, T. Yamazaki, KEK, Oho, Tsukuba, 305-0801, Japan
K. Ishida, RIKEN, Hirosawa, Wako, 351-0198, Japan
G.M. Marshall, TRIUMF, 4004 Wesbrook Mall, Vancouver V6T 2A3, Canada

Abstract

We have developed an ultraslow muon simulation as part of the project to measure the muon anomalous magnetic moment at the Japan Proton Accelerator Research Complex (J-PARC). The experiment will be conducted at a new muon beam line (H-line) at the Materials and Life Science Facility (MLF) in J-PARC. The H-line provides surface muons that thermalize in a silica aerogel target to form muonium. The generated muonium atoms are ionized by laser, to produce ultraslow muons. The ultraslow muons are extracted by an electrostatic accelerator and injected into a muon linac. This paper describes the simulation of the surface muons, muonium production, and electrostatic acceleration.

INTRODUCTION

Though the discovery of the Higgs boson at the large hadron collider (LHC) completed the particles predicted in Standard Model (SM) of elementary particle physics, some observations such as the existence of dark matter indicate new physics beyond SM at some energy scale or interaction scale. One of the clues for new physics is the anomaly of the muon anomalous magnetic moment $a_\mu = (g_\mu - 2)/2$; a difference of approximately three standard deviations exists between the SM prediction and the measured value (with a precision of 0.54 ppm) of a_μ [1]. Measurement with a higher precision is necessary to confirm this anomaly. Low-emittance muon beams will facilitate more precise measurements because the dominant systematic uncertainties in the previous experimental results are due to the muon beam dynamics in the muon storage ring.

The E34 experiment at the Japan Proton Accelerator Research Complex (J-PARC) [2] aims to measure a_μ with a precision of 0.1 ppm. The experiment uses a proton beam from the 3-GeV synchrotron ring to the Materials and Life Science facility (MLF). The proton beam is injected to a graphite target [3] to produce surface muons. The generated surface muons are extracted to a muon beam line called the H-line [4]. The surface muons stop in a silica aerogel target, and a portion of the muons form thermal muonium atoms (Mu, $\mu^+ e^-$) [5]. The Mu may be emitted following diffusion from the silica into a vacuum region, where the electron in the Mu is knocked out by laser ionization, and ultraslow muons (i.e., with a room temperature thermal distribution of typically 25 meV) are generated.

The generated ultraslow muons are electrostatically accelerated to 5.6 keV and injected to a muon linac. The accelerated muons are stored in a high precision muon storage magnet [6], where the time dependence of decay positrons is measured to reveal the muon spin precession frequency. Because the intensity of the ultraslow muons determines the statistical reach of the experiment, the intensity should be evaluated through dedicated simulations.

This paper describes simulations of H-line, Mu production and diffusion, and the electrostatic acceleration of the ultraslow muons.

SURFACE MUON BEAM LINE

Figure 1 shows the optics design of the H-line. The H-line beam is extracted at an angle of 60° in the forward direction. There is another muon beam line (D-line) on the opposite side of the proton beam. The front-end solenoid magnet (HS1) consisting of eight coils provides a muon capture field and transports the muons to the first bending magnet (HB1) which selects the beam momentum. The second and third solenoid magnets (HS2 and HS3) provide weak focusing fields in directions opposite to each other. A Wien filter is applied between HS2 and HS3 to eliminate positrons in the beam with momentum selected for muons. The second bending magnet (HB2) is placed to extract the beam if desired to another experimental area where some experimental programs [7, 8] are scheduled. For the a_μ experiment the surface muons are focused to the muonium production target by the quadrupole triplet after the fourth solenoid magnet (HS4).

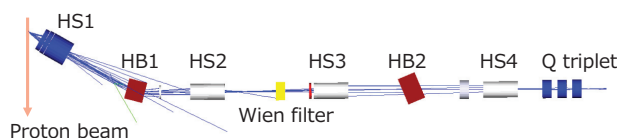


Figure 1: Optics design of H-line. Blue lines show a typical result for the transport of surface muons.

The surface muon production properties at the proton target were estimated using measurements at the D-line to avoid discrepancies among the hadron production models [9–11]. The D-line simulation was developed using the simulation package G4beamline [12]. The spatial distributions ($\sigma_x = 2$ mm and $\sigma_y = 4$ mm) were determined based on the proton beam profiles. The momentum distributions were

* masashio@post.kek.jp

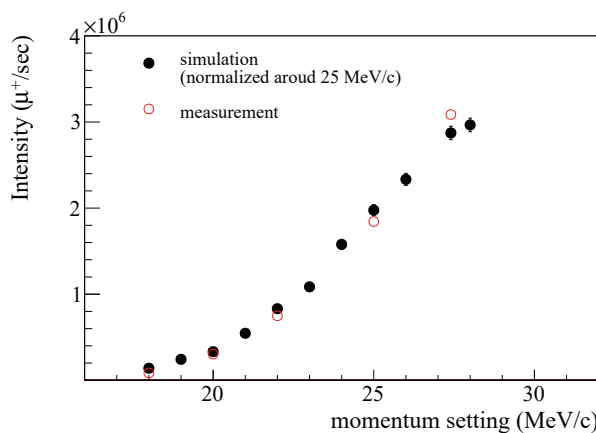


Figure 2: Momentum dependence of the surface muon intensity. Black and red circles show simulation and measurement results, respectively. The vertical scale of the simulation is normalized by the measured value around 25 MeV/c.

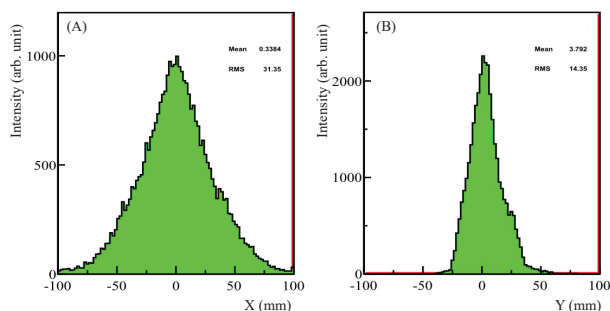


Figure 3: Estimated profiles at the muonium production target: (A) profile in the horizontal direction; (B) profile in the vertical direction.

implemented with the range of muons in the target material, graphite. Figure 2 shows the momentum dependence of the muon intensity at the D-line. There is good agreement between the measurement and simulation result. The surface muon intensity from the proton target was determined based on this result for the H-line simulation. The estimated muon intensity at the proton target is $2.0 \times 10^9/s$.

The G4beamline simulation for the H-line was developed to estimate the surface muon intensity and profiles at the muonium production target. In the simulation, the magnetic fields calculated by OPERA [13] were implemented. The current of each magnet is first tuned based on the experience of operating muon beam lines such as the D-line, following which the optimization algorithm of SIMPLEX [14] is applied so that the intensity at the muonium production target is maximized. Figure 3 shows the estimated profiles at the muonium production target. The profile widths in the horizontal and vertical directions differ from each other because the beam line is not free from momentum dispersion. The ratio of transportation efficiencies between H-line and D-line is estimated to be eleven. The muon intensity is estimated to be $3.2 \times 10^8/s$ at the muonium production target.

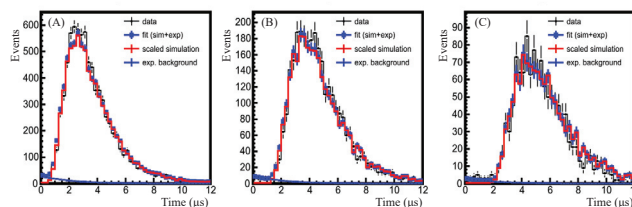


Figure 4: Fit of the diffusion simulation to emission data. (A) decay-time distribution in a region from 10 mm to 20 mm from the Mu production target; (B) from 20 mm to 30 mm; (C) from 30 mm to 40 mm. The black histogram shows the data, and the fit is shown by blue squares. The fit is the sum of the scaled simulation (red histogram) and an exponential background (blue histogram).

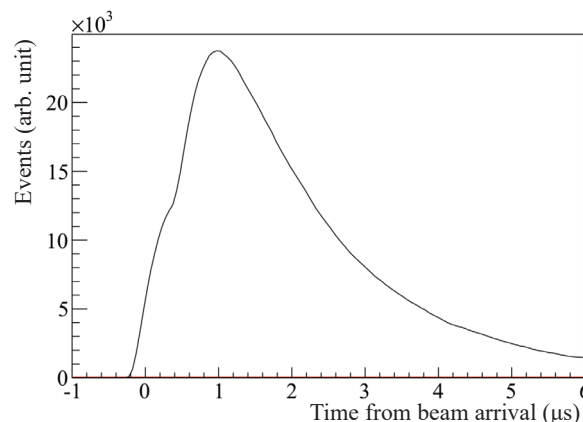


Figure 5: Number of ultraslow muons in the laser ionization region as a function of time since the average time of arrival of the muon beam.

MUONIUM PRODUCTION

A Mu production simulation is developed to estimate the Mu amount in the laser ionization region. The surface muon beam distributions described in the previous section were used as input. The muon stopping distributions in the silica aerogel target were estimated using GEANT4 [15]. A fraction of 52% of muons stopped in aerogel form Mu [16]. The simulation for muonium diffusion in the target is based on a three-dimensional random walk in which each step is taken with a speed derived from a Maxwell thermal distribution and a mean free path. The simulation parameters of the thermal temperature and the diffusion constant were determined from our measurement at TRIUMF [5]. Figure 4 shows a comparison between the measurement and the simulation after fitting the simulation parameters. There is a good agreement between the measurement and the simulation.

Figure 5 shows the number of ultraslow muons in the laser region as a function of time since the average time of arrival of the surface muon beam. The muon beam has a periodic time structure, with two pulses of width ~ 100 nsec separated by 600 nsec arriving with repetition rate of 25 Hz. The laser pulse duration to maximize the number of ultraslow muons is determined to be 1 μ sec.

Content from this work may be used under the terms of the CC BY 3.0 licence (© 2018). Any distribution of this work must maintain attribution to the author(s), title of the work, publisher, and DOI.

In summary, we calculated the efficiency of producing muonium atoms in the laser ionizing region at the time of the laser pulse. The fraction in the ionizing region is 3.8×10^{-3} . The laser ionization efficiency is based on a calculation assuming individual rates of induced emission and absorption as well as spontaneous photon emission [17]. The ionization efficiency is 0.73 for 100 μJ of Lyman- α (1S to 2S) radiation and 300 mJ ionization (2S to continuum) radiation.

ELECTROSTATIC ACCELERATION

An Soa lens [18] is employed for initial acceleration of ultraslow muons. The Soa lens consists of two mesh electrodes and three cylindrical electrodes. The first mesh electrode covers the downstream surface of the silica aerogel target. The laser ionization region is between two mesh electrodes. The acceleration voltage of the lens is set to 5.6 keV, corresponding to the RFQ input energy. The dimensions of the electrodes were designed to achieve a sufficient extraction efficiency for ultraslow muons. The electrostatic field of the Soa lens is calculated by OPERA. By using the Soa electric field and ultraslow muon distributions described in previous sections, the transmission efficiency is estimated by the GEANT4 simulation. Figure 6 shows a typical result of particle tracking.

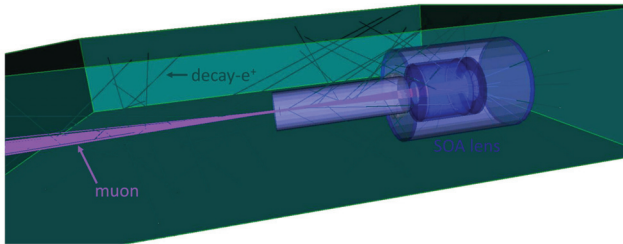


Figure 6: Typical result of particle tracking by the GEANT4 simulation. Purple shows muons and dark blue shows decay positrons.

Figure 7 shows phase space distributions at the entrance of the RFQ. The difference between the horizontal and vertical directions resulted from the difference of the surface muon distributions. The transmission efficiency is estimated to be 72% including a decay loss of 17%. The transmission efficiency of the mesh electrodes was evaluated to be 78% by the mesh aperture ratio.

The red-hatched ellipses in Fig. 7 show the design acceptance of the RFQ. The transmission efficiency of the RFQ is estimated to be 81% including decay loss [19] by using PARMTEQM [20]. The transmission efficiency of downstream components such as an inter-digital drift tube linac can be found in [21–24].

SUMMARY

We have developed the simulations of the H-line muon beam, Mu production and diffusion, and electrostatic acceleration for the J-PARC g-2 experiment. Table 1 summarizes the efficiency and muon intensity in each step. The muon

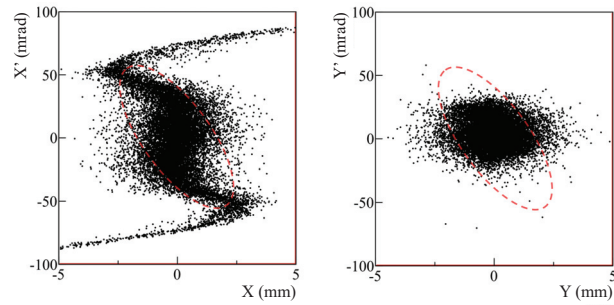


Figure 7: Phase space distributions at the entrance of the RFQ. The left figure shows the distribution for x, and the right figure shows that for y. The red-hatched ellipses show the design acceptance of the RFQ.

intensity at the entrance of the muon linac is estimated to be 5.0×10^5 /s. The acceleration of the muon linac, injection to the storage magnet, and other details can be found in [19,21–24]. We can measure the $(g_\mu - 2)$ anomaly with the same statistical sensitivity as in the previous experiment [1]. Because of the different experimental approach, the dominant systematic uncertainties in the previous experiment are negligible in our experiment. Further developments for higher muon intensity are being conducted to achieve the target sensitivity.

Table 1: Estimated Efficiency and Remaining Beam Intensity in Each Step

Step	Efficiency	Intensity (Hz)
μ^+ at production target		2.0×10^9
H-line transmission	0.16	3.2×10^8
Mu emission	3.8×10^{-3}	1.2×10^6
Laser ionization	0.73	9.0×10^5
Metal mesh	0.78	7.0×10^5
USM transmission	0.72	5.0×10^5

ACKNOWLEDGEMENT

This work is supported by JSPS KAKENHI Grant Numbers JP15H03666 and JP18H03707. We also acknowledge support from the Natural Sciences and Engineering Research Council of Canada (NSERC) Discovery Grant SAPPJ-2015-00039.

REFERENCES

- [1] G. W. Bennett *et al.*, *Phys. Rev. D* **73**, p. 072003 2006.
- [2] <http://g-2.kek.jp/portal/index.html>
- [3] S. Makimura *et al.*, *JPS Conf. Proc.* **8**, p. 051002 2014.
- [4] N. Kawamura *et al.*, *JPS Conf. Proc.* **2**, p. 010112 2014.
- [5] G. A. Beer *et al.*, *Prog. Theor. Exp. Phys.* **091**, p. C01, 2014.
- [6] M. Abe *et al.*, *Nucl. Instr. Meth. A* **890**, p. 51-63 2018.
- [7] Y. Nakatsugawa for DeeMe collaboration, *Nucl. Part. Phys. Proc.* p. 273-275, 1692-1698 2016.

- [8] H. A. Torii for MuSEUM collaboration, *JPS Conf. Proc.* **8**, p. 025018, 2015.
- [9] HARP Collaboration 2008, *Eur. Phys. J. C* **53** p. 177, 2008.
- [10] A. Ribon *et al.*, IEEE Nuclear Science Symposium Conference Record, IEEE, Orlando, FL, 2009.
- [11] A. Ribon *et al.*, CERN, Geneva, Switzerland, Technical Report no. CERN-LCGAPP, 2010.
- [12] G4beamline, <http://public.muonsinc.com/Projects/G4beamline.aspx>
- [13] OPERA3D, Vector Fields Limited, Oxford, England., <https://operafea.com/>
- [14] F. James and M. Roos, “Minuit: A System for Function Minimization and Analysis of the Parameter Errors and Correlations,” *Comput. Phys. Commun.*, vol. 10, pp. 343–367, 1975.
- [15] GEANT4, <http://geant4.cern.ch/>
- [16] P. Bakule *et al.*, *Prog. Theor. Exp. Phys.* **103**, C01, 2013.
- [17] See, for example, H.A. Bethe, and E.E. Salpeter, “Quantum Mechanics of One- and Two-electron Atoms”, Sect. 68, Springer-Verlag, Berlin 1957.
- [18] K. F. Canter *et al.*, *Positron studies of solids, surfaces and atom*, p. 199, World Scientific, Singapore, 1986, and *Nucl. Instr. Meth. B* **266**, 335 2008.
- [19] N. Saito, and R. Kitamura, in *Proceedings of IPAC2015*, Richmond, VA, USA, 2015, pp. 3801–3803, and Y. Kondo *et al.*, in *Proceedings of IPAC2015*, Richmond, VA, USA, 2015, pp. 3801–3803.
- [20] K. R. Crandall *et al.*, “RFQ Design Codes”, LANL, Los Alamos, NM, USA, Report no. LA-UR-96-1836 1996.
- [21] M. Otani *et al.*, *Phys. Rev. Accel. Beams* **19** p. 04010 2016.
- [22] M. Otani *et al.*, in *Proceedings of IPAC2016*, Busan, Korea, pp. 1543–1546, 2016.
- [23] Y. Kondo *et al.*, *J. Phy. Conf. Ser.* **874**, p. 012054, 2017.
- [24] H. Iinuma *et al.*, *Nucl. Instr. Meth. A* **832**, p. 5162 2016.